A Benchmark for Automated Vickers Hardness Testing

E. Jalilian[1 [0000−0001−5925−5735]] and A. Uhl[1 [0000−0002−5921−8755]]

Department of Artificial Intelligence and Human Interfaces (AIHI) of the University of Salzburg, Salzburg, 5020, Austria {ejalilian, uhl@cs.sbg.ac.at}@cs.sbg.ac.at
http://www.plus.ac.at

Abstract. Automated Vickers hardness measurement methods must be robust and versatile to cope with materials with rough and noisy patterned surfaces. The behaviour of several state-of-the-art algorithms for automated Vickers hardness measurement is evaluated and compared for their respective robustness and accuracy. The evaluation is based on real world industrial data, collected in a Vickers indentation dataset. Addressing the current lack of publicly available (annotated) Vickers indentation data, and in order to provide a benchmark for further investigations and experiments, we release the databases used in this work, together with expert groundtruth covering diagonal measurement and segmentation masks, and make them available on-line for public open access.

Keywords: Vickers Hardness Testing · Deep-learning · Automated Vickers Hardness Measurement.

1 Introduction

Vickers Hardness measurement is a nondestructive test with wide application in industrial manufacturing processes, in which the resistance of solid materials such as metal, ceramic, polymer, etc, is examined against the penetration of an indenter. In this process, hardness testing machines called durometers are use to force a pyramidal diamond indenter with an angle of 136°between opposite faces on the specimens' surface. According to international standards [1], the measurement process is carried out by determining the lengths of the diagonals of the approximately square shaped indentation and calculating the Vickers hardness (VH) value from the average of the diagonals and the applied force:

$$VH = \frac{1}{g}\ \frac{2Fsin\frac{136^\circ}{2}}{d^2}, \tag{1}$$

where F is the applied force, d is the mean of the diagonal length of the indentation, and g is the acceleration of gravity (see Figure 1 for an illustration). Manual inspection and measurement of indentations is time consuming (approximately 2 min 3 per indentation [27]) and very interpretive, subject to the

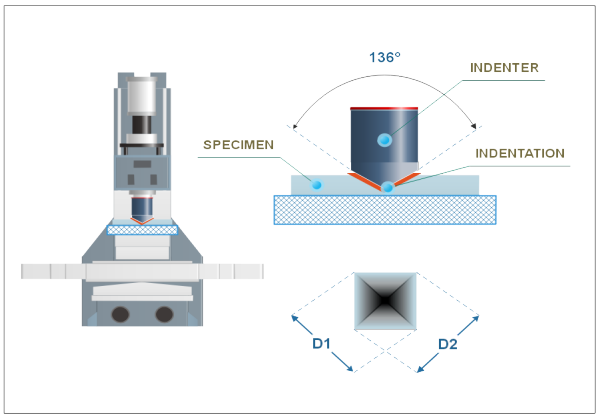

Fig. 1: Durometers and Vickers indentation hardness test schematics

operator's experience and observation conditions [25]. Automated hardness testing systems, which utilize image processing techniques, have been developed to address these issues and also to provide more accurate measurements. Accurate localization and detection (i.e. segmentation) of the indentation contour in the indentation images is the most crucial step for the correct measurement of the indentation dimensions. Such images are captured from diverse materials on different machines and at changing environmental conditions (*i.e.* illumination, focus, magnification, ...). So, the indentations vary significantly in terms of: Size, location, rotation, brightness, contrast, and texture characteristics. Additionally, the target specimens typically have noisy surfaces which contain cracks, sparkles and other distortions resulting from industrial processes applied to the material surface. Thus, typical image processing methods often fail to detect indentations due to such properties.

In this work we evaluate the performance of four typical algorithms proposed for automated Vickers hardness measurement and compare their measurement performance, where the algorithm proposed in [20] is evaluated for the first time on a larger dataset. As a major contribution, we introduce a Vickers indentation database collected from real world industrial data. We release the database to the public and make it available online along with the ground truth information, addressing the current lack of publicly available (annotated) Vickers indentation data, also providing a benchmark for further investigations and algorithm developments. The database and metrics are described in Sec. 3, while Sec. 4 explains the algorithms and methodologies. Experiments and results achieved are presented in Sec. 5, and Sec. 6 concludes the paper.

2 Related Works

Several methods have been proposed for automated indentation detection and measurement. Thresholding algorithms are frequently used to segment the indentation area [24], applying various approaches such as: Using a predetermined threshold level together with a four-neighborhood algorithm to remove speckles [17], determining the threshold level from histogram separation [27], using a modal threshold and morphological closing [21], or using the Johannsen algorithm to identify the threshold level [25]. Determining a threshold level based on the global image grayscale distribution is very difficult, as brightness and contrast varies between images, defects are often darker than the indentation and the contrast of the indentation can be lower than global image contrast variations.

Edge detection algorithms applied aim to detect the vertex points of the indentation directly. For instance, a Sobel operator and minimum/maximum detection has been used to find corner points of indentations [13]. Ray sweeping, edge tracing [3], line Hough transform [23], and edge/vertex template matching are further algorithms proposed from the same algorithmic class. Due to their often local application, the output of vertex detection is often faulty and algorithms are misled by crossing break-lines, and speckles in the rough-polished specimens. Also, although quite effective in terms of accuracy, the template based algorithms exhibit performance problems due to an exhaustive number of match operations, and requirements for orientation alignment.

One group of algorithms relies on wavelet analysis [15]. These methods assume that object borders are perfectly straight lines, which is not always true. Axes projection algorithms locate the indentation by searching for significant differences in the sum of row or column values of the image. Axes projection can either be applied to the gray level image directly [30] or the image can be binarized beforehand by thresholding [27]. Nevertheless, this approach suffers some serious drawbacks. Basically, very small indentations lack significant markers. Also, in order to obtain strong markers, the indentation must be reasonably aligned in x,y-direction in the projections. However, often the indentations are rotated by 45 degrees or do not have proper alignment at all.

A specific class of algorithms use multi-resolution approaches to increase robustness and speed of the vertex detection process [5] [7] [6] [8]. These algorithms either apply template matching for indentation detection, edge approximation and vertex determination [5], or use shape prior gradient descent and level set active contour methods for the segmentation [7] [6] [8]. The use of unfocused images shows a positive influence on the indentation localisation process whether these images are used directly [4] or a shape from focus approach is used to recreate the indentation first [8]. The major problem of the above mentioned algorithms is that they perform excellently only on a large subset of indentation images while real world indentation imagery still exhibits some image properties which are problematic for those algorithms. Especially early algorithms are susceptible to indentation images with strong specimen surface texture or dominant artifacts. The indentation recognition rate as well as the vertex measure-

ment accuracy are clearly increased in these approaches, expanding the range of processable indentation images but there are still scenarios where problematic images occur. High dimensional texture feature vectors which are constructed from the fractal dimension of image regions as well as the energy and entropy of co-occurrence matrices are used in [9]. There are further techniques which use a combination of the above mentioned techniques or other classical image processing techniques [24].

Recent advances in machine learning and deep-learning techniques (*e.g.* Convolutional Neural Networks (CNNs)) have motivated a number of researchers to utilize the feature extraction power of convolutional neural networks to tackle the challenging task of indentation detection and localization. Not focussing directly on image analysis, but using the mechanical properties of a solid (bulk modulus, shear modulus, Young's modulus, and Poisson's ratio) as input variables in a Gradient Boosting Regressor (GBR) schema to predict hardness is proposed in [2]. In another work [22], the performance of four distinct neural network architectures: Multilayer Perceptron (MLP), Convolutional Neural Network (CNN), Long Short-Term Memory network (LSTM), and Transformer for the precise prediction of Vickers hardness in nitrided and carburized M50NiL steel samples is evaluated [14].

A method for the detection of Brinell indentation edges using CNNs has been reported in [28], where the outcomes showed promising results. However, there are some issues unique to the Vickers indentations. In particular, the diagonal length of the indentation is much smaller than with Brinell, and crackings that sometimes occur during Vickers hardness testing do not occur in Brinell hardness testing. A recent work [29] used a CNN network to specify the bounding box containing the Vickers indentation, and then used a subsequent CNN for detecting the left vertex position of the indentation. Similarly in [14], authors proposed a two-steps approach in which a rough location method based on morphological processing is first used to obtain the approximate range of the indentation and crop it out from a given image. Then, a CNN (U-net [26]) is used to predict the mask of the indentation in the cropped image. To this extent, these more recent models also lack the required speed and accuracy. In [12] a Fully Convolutional Neural network (FCN) is chosen to accurately localize and segment the Vickers indentations. A set of liner curves are then fitted to the boundary pixels data extracted from the output segmentations. The initial positions of the indentation vertices are estimated as the cross-sectional point of adjacent boundaries to each indentation vertex. A complimentary segmentation module then is used to refine the target regions, and accurate indentation vertices positions are then calculated applying further geometric processing steps.

3 Database and Metrics

3.1 Vickers indentation database

A properly sized database of representative Vickers indentations images is made publicly available[1]. The database serves as a foundation for the evaluation of Vickers indentation processing algorithms. The database is composed of two data sets in which 150 images are included in DB-I and 216 images in DB-II. Manual measurement data created by hardness testing experts are provided for each image as the ground truth for algorithm result assessment. To our best knowledge, this is the first time that such a database is made available.

All images have been taken from camera equipped hardness testing machines in industrial production environments. Each machine has an optical microscope that offers ten- to hundredfold magnification of the specimen and a monochrome CCD camera that produces 8-bit grey scale images at a resolution of 1280 x 1024 pixels. Although originally in JPEG format, the images have been converted to PNG format during collection from the system. A flaw of the camera system is that the border pixels of the image can be damaged an shall thus be ignored.

Indentation images for the database are selected to provide a wide range of variety and to include a reasonable number of challenging surfaces (see Fig. 2 for examples), however they always show exactly one Vickers indentation. The images have a significant variation in size, position and rotation of the indentation, the texture of the specimen and the contrast of the picture.

3.2 Ground truth Derivation and Result Metrics

The Vickers hardness is determined from the indentation area, which in turn is calculated from diagonals by implying, that the area of the indentation has a square shape [1]. This disregards the fact, that the indentation is rarely a perfect square and thus the diagonals are only an approximation of the area. Nevertheless, it is the established approach for the Vickers hardness and the way manual measurement is carried out. In expert practice, perpendicular measurement line are positioned to attach to the vertices of the indentation. The measurement lines can be rotated, if the indentation is rotated likewise.

Manual measurement is carried out by an operator attaching measurement lines to the indentation as shown in the leftmost image of Fig. 3. If necessary, theses lines are rotated to mimic a rotation of the indentation in the image. The distances of corresponding measurement lines give the diagonals, which are further used for the calculation of the hardness value. To achieve stable results, the measurements have been carried out not only by one person but by a number of hardness testing experts. DB-I has been measured by four and DB-II by five different people. These independent measurements show surprisingly high variations in the position and the rotation of the measurement lines and thus the lengths of the diagonals.

[1] `https://wavelab.at/sources/Jalilian24a`

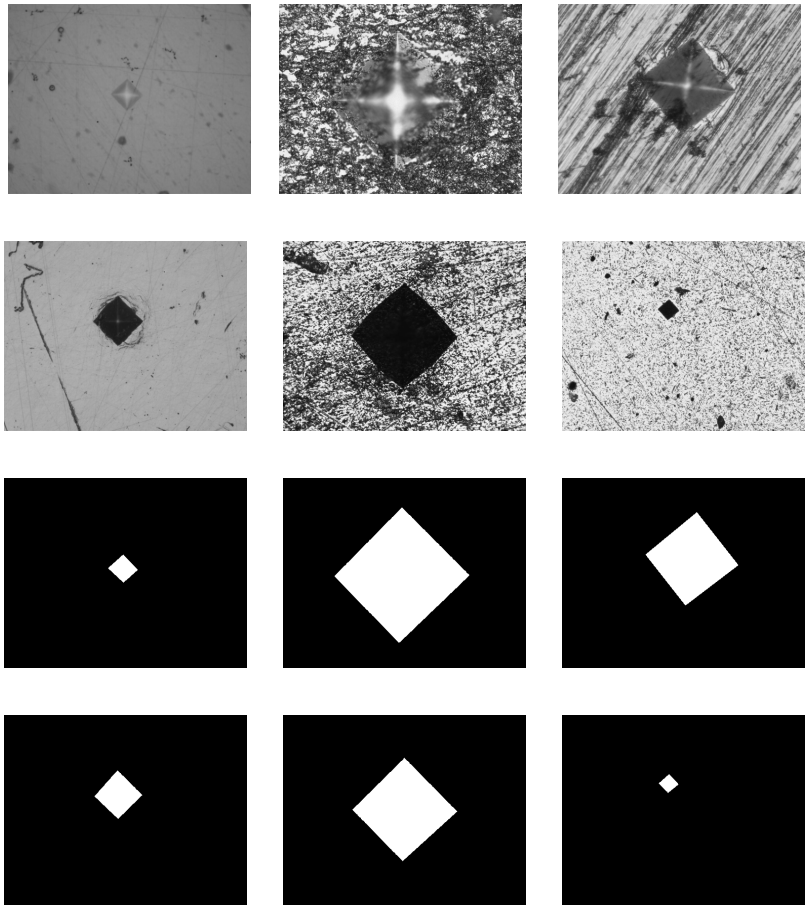

Fig. 2: Sample indentation images in the dataset DB-I (first row) and the dataset DB-II (second row), and their corresponding ground truth masks (the second and the third row) respectively

The ground truth for each diagonal is then defined to be the median of the measurements of the experts. This ground truth is used throughout the paper to determine the accuracy of the studied algorithms by looking at the histogram of the deviations. Furthermore, from the image processing point of view not only the correct length of the diagonals is important but also the location of a calculated vertex in relation to its supposed position. Because of the varying orientations of the manual measurement lines such displacements are complicated to determine (see Fig. 3). The method that is used is to compute the average of the orientations of all measurement lines to project a perpendicular line through the vertex. This perpendicular line intersects the measurement lines. From these intersections the median distance to the vertex is used to assign a candidate line. For this

candidate line the distance in pixels to the vertex is set as the deviation of the vertex.

A similar approach is to be taken when rating vertex positions of the vertices produced by the automated indentation measurement algorithms against ground truth. The (rounded) median distance of a vertex to the corresponding manual measurement lines is computed as the error metric. It should be emphasised, that the ground truth does not specify vertex positions but bounding boxes to the indentations, so absolute vertex positions errors can not be obtained. It is also worth to mention that many of our previous investigations already done on the topic such as: [3] [5] [6] [7] [8] [4] [18] [19] [20] [12] contain results relative to the datasets and the ground truth information released with this paper.

3.3 Indentation Area Manual Ground truths

Supervised learning methods are the backbone of many algorithms newly proposed to address the key artificial vision challenges such as image segmentation and feature extraction. In order to train such models, the input data needs to be accompanied by manually labeled masks (ground truth data), which in fact supervises the model to learn the target features. Addressing this need, we generated two sets of ground truth data for both datasets. For this purpose we used an image labeling tool to articulate the indentation pixels using two approaches: In the first approach, the indentation pixels are marked by fitting a rectangle-shaped mask to the indentation vertexes. While this approach provides a good approximation of the indentation area, yet, due to the fact that the actual indentations' borders have rather concave or convex profile, in some cases the fitted mask on the indentation areas includes some background (surface) pixels or vise versa. To address this, in the second approach we attach polygon vertices to the indentation borders points, generating more precise ground-truth masks. As a further contribution of this paper, both ground truth sets are made publicly available[2] as well. Fig. 2 demonstrates examples of the Vickers indentations images in the datasets, and their corresponding ground truth masks.

[2] `https://wavelab.at/sources/Jalilian24a`

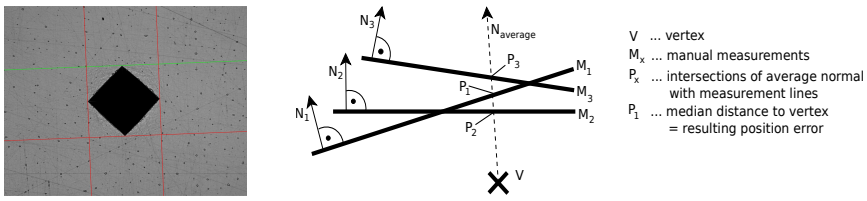

Fig. 3: Measurement lines from manual measurement and determination of vertex displacement error

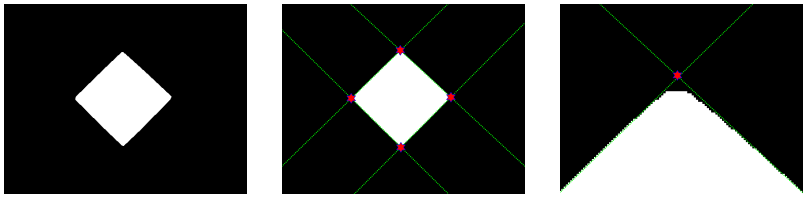

Fig. 4: A sample indentation CNN output segmentation (left), the curves fitted to the indentation four edge points (middle), and an initial vertex position specified (right)

4 Algorithms and Methodologies

Four state-of-the-art algorithms for automated Vickers hardness measurement are evaluated and compared for their measurement performance to foster the development of a reliable benchmark. In particular, a deep-learning algorithm and three classical methods are examined in this work.

4.1 Deep-learning Based Algorithm

Addressing the drawbacks of classical segmentation methods and reducing the complexity of intensive pre- and/ or post-processing steps, deep-learning techniques (*i.e.* Convolutional Neural Network (CNN)) are driving major advances in automated object recognition and segmentation. The models proved to provide superior performance in wide variety of applications, specially in complicated and challenging segmentation tasks [10] [11]. As we already mentioned, the key challenging step in automatic Vickers indentation testing is robust localization and segmentation of the indentation in the images. So, a segmentation Deep-learning based (DL) CNN is selected to handle this task [12].

RefineNet [16] is a multi-resolution refinement segmentation network, which employs a 4- cascaded architecture with 4 Refining units, each of which directly connects to the output of one Residual net [14] block, as well as to the preceding RefineNet block in the cascade. Each Refining unit consists of two residual convolution units (RCU), which include two alternative ReLU and 3×3 convolutional layers. The output of the RCU units are processed by 3×3 convolution and up-sampling layers incorporated in multi-resolution fusion blocks. A chain of multiple pooling blocks, each consisting a 5×5 maxpooling layer and a 3×3 convolution layer, next operate on the feature maps, so that one pooling block takes the output of the previous pooling block as input. The outputs of all pooling blocks are fused together with the input feature maps through summation of residual connections.

In [12], we leveraged the segmentation power of the RefineNet to get the challenging task of indentation positioning and segmentation accomplished. However, the corner regions pixels went missing in the output segmentations (see Fig. 4

for an example). Missing corner pixels is a general segmentation issue and is not specific to the CNN-base segmentation models, however, these are extremely important for accurate measurements of the diagonal length. So, we aim to improve the initial vertices position estimations. This leads to a hybrid approach, combining the robustness and generalisability of deep-learning based semantic segmentation networks with the high pixel-wise accuracy of many classical techniques. For doing so, we first extract the indentation contour points from the segmentation outputs, and fit a first degree polynomial curve into each indentation boundary curve utilizing a least-squares criterion. Next, the intersection point of each two crossing curves are calculated to determine the initial coordinates of the indentation vertices (see Fig. 4). A 40×30 window is defined around each initial vertex position as region of interest (ROI), and an automated thresholding algorithm (Otsu's) is applied to this region. See Fig. 5 for an illustration of this segmentation process.

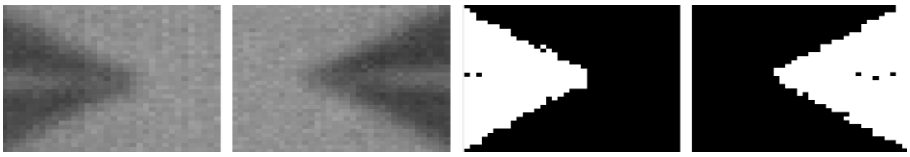

Fig. 5: A sample's right and left ROI images and their corresponding output segmentations as obtained by the Otsu procedure.

The final vertex positions then are specified as the coordinate of the most extreme pixels located at the tip of the segmented indentation region within the ROIs [12].

4.2 Classical Model-based Algorithms

In addition to the DL algorithm, three classical algorithms from different domains are used:

The **ALG (AreaMap-LogPolar-Gabor) algorithm** [20] uses the AreaMap operator [19] for indentation localization. The operator takes advantage of the uniformity of the brightness distribution gradients of an indentation compared to its surroundings. For each pixel in the image, the area of the pixels reachable by monotonic descending brightness (DecAMap) or ascending brightness (IncAMap) is calculated. The pixel with maximum reachable area is taken as an inner point (but not necessarily the center) of the indentation. The inner point is used as the pole for a log-polar transformation of the image. See Fig. 6 for two examples of indentation images and their log-polar representation.

In log-polar space, a single fixed template can robustly identify the edges of the indentation, utilizing that the log-polar transformed image decreases the effect of surface artefacts. The edges are then used to calculate good approximations for the indentation center, size and orientation. In Fig. 7 we illustrate

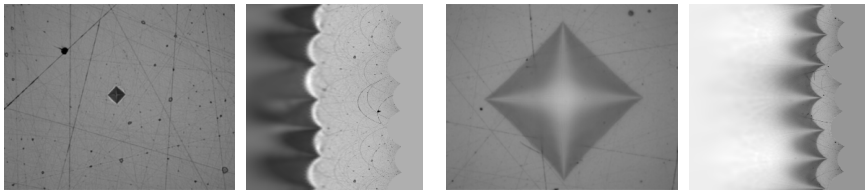

Fig. 6: Example of indentation images and their log-polar representations.

the stages of this process which ends by providing the edge position. The match exhibits four distinct maxima at the positions of the edges. These maxima are horizontally aligned and equally spaced in the vertical direction, therefore a fixed filter can be used to detect them. The applied filter operation is actually another normalized cross-correlation of the filter with the match. Back-projecting the positions of the filtered maxima into the original image identifies the midpoints of the indentation edges while backprojecting to the log-polar space gives the rotation of the indentation.

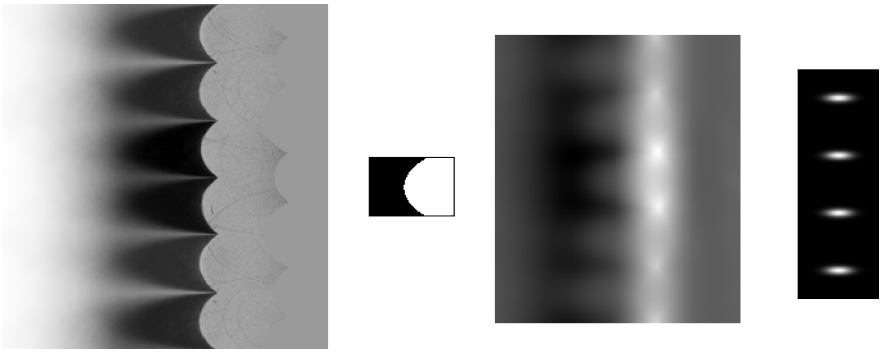

Fig. 7: Example log-polar image, edge template, matching result and edge position filter.

This information is used in the indentation image to guide modified cascading Gabor filters on vertex adjoining edges. The Gabor filters perform a coarse-to-fine approximation on the edges and the intersection of the edges define the indentation vertices as illustrated in Fig. 8.

The Gabor filters are used in the proximity of vertices to approximate the adjacent edges. For that reason a filter is split into two halves from which only one half is applied to a respective edge while the other half is ignored. The origin of the filter is placed at the estimated vertex position and allowed to move perpendicular to the direction of the edge in a limited range to improve the filter response. The best filter response is taken as the new vertex position

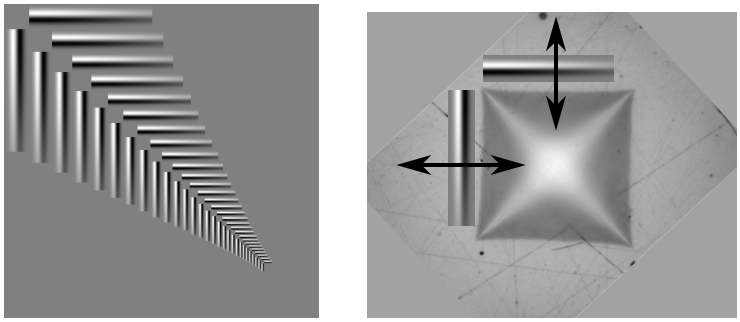

Fig. 8: Gabor half-filter cascades and principle of operation for the upper left vertex.

which itself serves as the vertex estimate for the next iteration. The next iteration starts after both adjacent edges have been processed. It uses scaled down Gabor filters and limits the range in which the filters are applied.

The **3SMRTM (3-stage multi resolution template matching) algorithm** [5] applies multi resolution template matching in three varying stages to identify indentation vertices. In the first stage, a template is used resembling a dark indentation square in a bright surrounding within a circular region. The indentation center is masked because it sometimes exhibits inverted brightness. The template is balanced, and offers orientation independent matching capabilities. It is used at four different angles and with fixed size, while the image is scaled from very small up to original size. On the way through the scaled images, the first significant maximum in the best match value is taken as the approximation of the image size, while the match position and match angle in the image approximate the location and rotation of the indentation. In the second stage, the position of the edges are refined with the help of rotation invariant line templates. To model a possible convexity or concavity of edges, a hypothetical joint in the middle is added and the location of each segment is computed from the best match with the (rotated) line template. In the last stage, a rotation invariant vertex template is rotated according to the orientation of the adjacent edges and and the best match in the surrounding of the intersection of the edges is determined as the indentation vertex position.

The **SPAC (Shape Prior, Active Contours) algorithm** [6] is again a three stage approach, but based on the idea of active contours. The first step uses a Shape-Prior method with a square shape outline to find the Vickers indentation. It applies forced shrinking of the shape while optimizing the shape position and orientation according to a specially crafted energy function. From the shrinking steps, the maximum match with an indentation template is taken as a size and location approximation of the indentation. The approximation is refined in the second stage with an region based level set method, where the energy function is calculated from the deviation of pixel brightness from the inner

Table 1: Diagonal indentation measurement results for different algorithms along with the corresponding manual measurements

Measure	Average Diagonal Error (pixels)		Non-outlier Average Diagonal Error (pixels)	
Database	DB-I	DB-II	DB-I	DB-II
DL	7.03	3.24	2.43	1.51
ALG	2.28	2.23	2.14	2.23
3SMRTM	6.37	4.87	2.86	3.00
SPAC	6.11	7.46	3.32	2.81
Manual measurements	3.12	4.28	3.06	4.30

and outer average. In the third step, the Hough transform of the shape in the proximity of the vertices yields straight lines, which are intersected to obtain the final vertex positions.

5 Experiments and Results

We applied all four algorithms to our datasets and used the median of the diagonal length measurements provided by the experts as the reference to determine the accuracy of the algorithms by inspecting the histogram of the deviations as presented in Fig. 9. In particular, we evaluated the overall algorithms performance in terms of two averages errors: The overall average errors (reflecting the algorithm robustness and accuracy), and the non-outlier average error in which the errors exceeding 20 pixels are suppressed (reflecting the algorithm precision). Table 1 lists the algorithms together with the results obtained in these experiments. Considering the primary measurement errors (non-outlier average diagonal errors), the DL algorithm shows superior performance on DB-II in comparison to the other algorithms (1.51 pixels error). However, the performance of the ALG algorithm is slightly better on DB-I when considering this error metric. The ALG algorithm maintains its supremacy on DB-I as well as on DB-II when considering the average diagonal error as well. In any case, the results as obtained by these two automated Vickers hardness measurement methods proved to be very precise on both datasets, as they are even better than the average manual measurements in almost all cases (except considering average diagonal error when applying the DL algorithm on the DB-I dataset). The 3SMRTM and SPAC algorithms show promising results on both datasets (specially DB-II) when considering non-outlier average diagonal errors as well. However, this does not apply to the DB-I dataset, and here, the accuracy of these two algorithms falls behind the manual measurements.

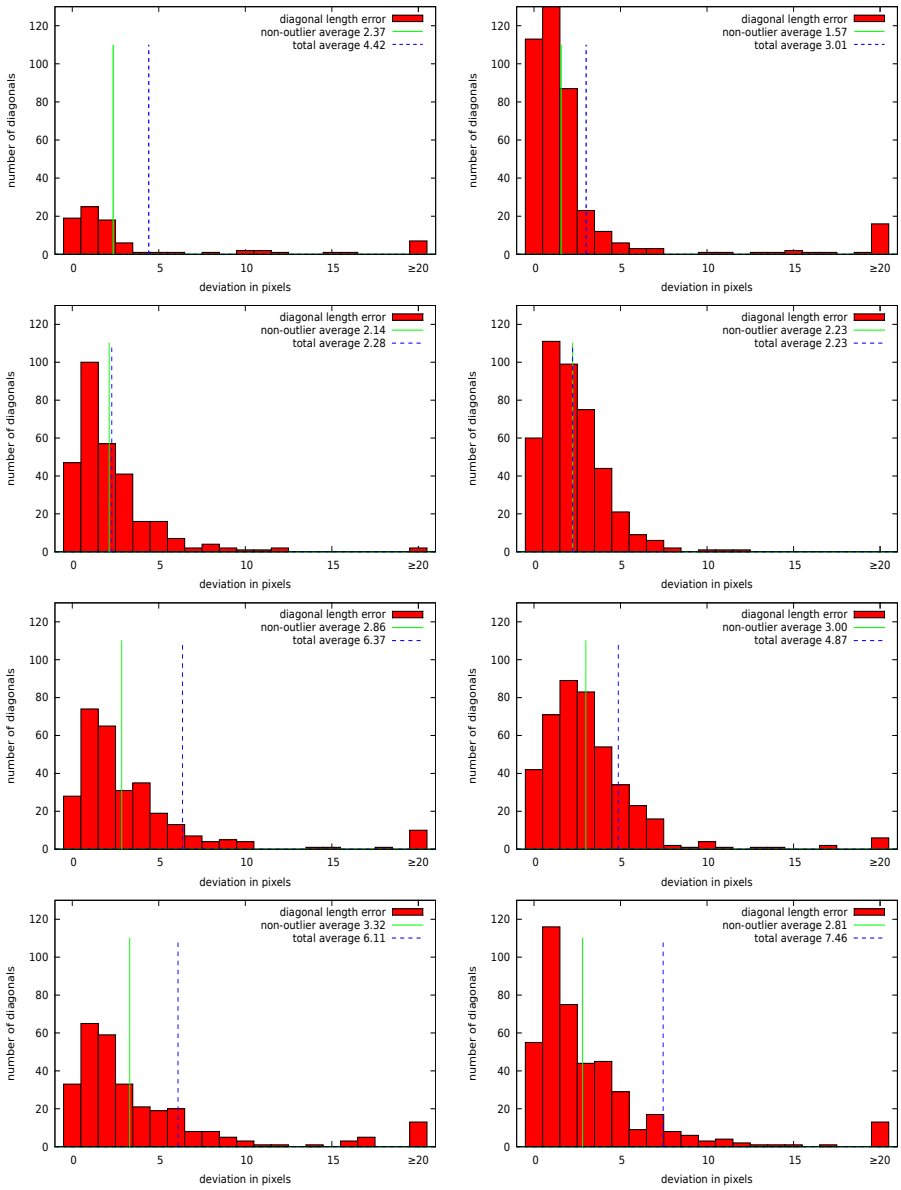

Fig. 9: Error of diagonal lengths in pixel using the DL (first row), ALG algorithm with brightness remapping (second row), 3SMRTM algorithm (third row) and SPAC algorithm (forth row) for the DB-I (left column) and DB-II (right column) datasets

6 Conclusion

Experimental results obtained in this work show that the more recently proposed automated Vickers hardness measurement methods (ALG and DL) are able to successfully tackle the challenging task of indentation localization and segmentation, especially in difficult cases where indentation profiles are distorted by rough specimen surface, sparkles, and low contrast. In case of the DL algorithm, absence of tuneable parameters in the algorithm avoids complicated preparation steps and makes it usable instantaneously. The 3SMRTM and SPAC algorithms also delivered promising results on both datasets, when considering non-outlier average diagonal errors. The properties of all four algorithms have been evaluated on two indentation image datasets, which include a substantial number of real world images taken at industrial environments. The size of the datasets enables the calculation of statistics, which give quantitative predictions about the viability of an algorithm when deployed. Thus, as one of the main objectives of this work, the evaluation results can be used as a reliable benchmark for further investigations and experiments on automated Vickers hardness measurement. To further endorse this objective, we release the datasets as used in this work along with the ground truth information (the manual diagonal measurements and the segmentation masks), and make them available on-line for open public access. Ever increasing eager to use deep-learning approaches, due to their supreme performance, and the need for manual ground truth information (masks) to train such modules highlights the importance of the availability of such ground truth annotation.

Acknowledgements This research was funded by the Salzburg State Government within the Science and Innovation Strategy Salzburg 2025 (WISS 2025) under the project AIIV-Salzburg (Artificial Intelligence in Industrial Vision), project no 20102-F2100737-FPR.

References

1. ASTM Standard E384, (2010e2): Standard test method for Knoop and Vickers hardness of materials. In: ASTM standards. ASTM International, West Conshohocken, PA (2010), `www.astm.org`, DOI: 10.1520/E0384-10E02, www.astm.org.
2. Dovale-Farelo, V., Tavadze, P., Lang, L., Bautista-Hernandez, A., H-Romero, A.: Vickers hardness prediction from machine learning methods. Scientific Reports **12**(1), 22475 (2022)
3. Gadermayr, M., Maier, A., Uhl, A.: Algorithms for microindentation measurement in automated Vickers hardness testing. In: tenth International Conference on Quality Control by Artificial Vision. vol. 8000, p. 80000M. International Society for Optics and Photonics (2011)
4. Gadermayr, M., Maier, A., Uhl, A.: The impact of unfocused Vickers indentation images on the segmentation performance. In: International Symposium on Visual Computing. pp. 468–478. Springer (2012)

5. Gadermayr, M., Maier, A., Uhl, A.: Robust algorithm for automated microindentation measurement in Vickers hardness testing. Journal of Electronic Imaging **21**(2), 021109 (2012)
6. Gadermayr, M., Maier, A., Uhl, A.: Active contours methods with respect to Vickers indentations. Machine Vision and Applications **24**(6), 1183–1196 (2013)
7. Gadermayr, M., Uhl, A.: Dual-resolution active contours segmentation of Vickers indentation images with shape prior initialization. In: Image and Signal Processing: 5th International Conference, 2012, Agadir, Morocco, June 28-30, 2012. Proceedings 5. pp. 362–369. Springer (2012)
8. Gadermayr, M., Uhl, A.: Image segmentation of Vickers indentations using shape from focus. In: International Conference Image Analysis and Recognition. pp. 149–157. Springer (2012)
9. Guitang, W., Jianlin, Z., Peiliang, C.: Application of fractal dimension and cooccurrence matrices algorithm in material Vickers hardness image segmentation. In: Proceedings of the 3rd International Conference on Intelligent Information Technology Application. IITA'09, vol. 3, pp. 624–627. IEEE Press, Piscataway, NJ, USA (nov 2009), http://dl.acm.org/citation.cfm?id=1794914.1795071
10. Jalilian, E., Uhl, A.: Iris segmentation using fully convolutional encoder–decoder networks. In: Bhanu, B., Kumar, A. (eds.) Deep Learning for Biometrics, chap. 6, pp. 133–155. Springer, (ZG) Switzerland (2017)
11. Jalilian, E., Uhl, A.: Finger-vein recognition using deep fully convolutional neural semantic segmentation networks: The impact of training data. In: Proceedings of the IEEE 10th International Workshop on Information Forensics and Security. pp. 1–8. Hong Kong (2018)
12. Jalilian, E., Uhl, A.: Deep learning based automated Vickers hardness measurement. In: Proceedings of the 19th International Conference on Computer Analysis of Images and Patterns. springer lecture Notes on International Conference, vol. 13053, pp. 3–13. Nicosia, Cyprus (held Online due to Covid) (2021)
13. Ji, Y., Xu, A.: A new method for automatically measurement of Vickers hardness using thick line hough transform and least square method. In: 2009 2nd International Congress on Image and Signal Processing. pp. 1–4. IEEE (2009)
14. Li, Z., Yin, F.: Automated measurement of Vickers hardness using image segmentation with neural networks. Measurement **186**, 110200 (2021)
15. Liming, W., Qu, Z., Yaohua, D., Miaoxian, Z.: Automatically analyzing the impress image of Vickers hardness test using wavelet. China Mechanics Engineering **15**(6) (2006)
16. Lin, G., Milan, A., Shen, C., D-Reid, I.: Refinenet: Multi-path refinement networks for high-resolution semantic segmentation. CoRR **abs/1611.06612** (2016)
17. Macedo, M., Berilli-Mendesand, V., Conci, A., R-Leta, F.: Using hough transform as an auxiliary technique for Vickers hardness measurement. In: Proceedings of the 13th International Conference on Systems, Signals and Image Processin (IWSSIP'06). pp. 287–290 (2006)
18. Maier, A., Uhl, A.: Robust automatic indentation localisation and size approximation for Vickers microindentation hardness indentations. In: 2011 7th International Symposium on Image and Signal Processing and Analysis. pp. 295–300. IEEE (2011)
19. Maier, A., Uhl, A.: The areamap operator and its application to Vickers hardness testing images. International Journal of Future Generation Communication and Networking **5**(4), 1–16 (2012)

20. Maier, A., Uhl, A.: Areamap and Gabor filter based Vickers hardness indentation measurement. In: 21st European Signal Processing Conference. pp. 1–5. IEEE (2013)
21. Mendes, V., Leta, F.: Automatic measurement of Brinell and Vickers hardness using computer vision techniques. In: Proceedings of the XVII IMEKO World Congress. vol. 3, pp. 992–995 (2003)
22. Niu, J., Miao, B., Guo, J., Ding, Z., He, Y., Chi, Z., Wang, F., Ma, X.: Leveraging deep neural networks for estimating Vickers hardness from nanoindentation hardness. Materials **17**(1) (2024), https://www.mdpi.com/1996-1944/17/1/148
23. Pan, Y., Shan, Y., Ji, Y., Zhang, S.: A new method for automatically measuring Vickers hardness based on region-point detection algorithm. Proceedings of the fourth International Symposium on Precision Mechanical Measurements **SPIE 7130**, 71304C–71304C–6 (2008)
24. Pedrosa, P., Filho, P.P., Cavalcante, T., Cavalcante, S., Hugo, V., Albuquerque, V., Tavares, J., Joao, P.: Brinell and Vickers hardness measurement using image processing and analysis techniques. Journal of Testing and Evaluation - J TEST EVAL **38** (01 2010)
25. Pedrosa-Rebouças-Filho, P., daSilveira Cavalcante, T., Hugo-deAlbuquerque, V., Manuel-RS-Tavares, J.: Brinell and Vickers hardness measurement using image processing and analysis techniques. Journal of Testing and Evaluation **38**(1), 88–94 (2010)
26. Ronneberger, O., Fischer, P., Brox, T.: U-net: Convolutional networks for biomedical image segmentation. In: International Conference on Medical Image Computing and Computer-assisted Intervention. pp. 234–241. Springer (2015)
27. Sugimoto, T., Kawaguchi, T.: Development of an automatic Vickers hardness testing system using image processing technology. IEEE Transactions on Industrial Electronics **44**(5), 696–702 (1997)
28. Tanaka, Y., Seino, Y., Hattori, K.: Measuring Brinell hardness indentation by using a convolutional neural network. Measurement Science and Technology **30**(6), 065012 (2019)
29. Tanaka, Y., Seino, Y., Hattori, K.: Automated Vickers hardness measurement using convolutional neural networks. International Journal of Advanced Manufacturing technology **109**(5), 1345–1355 (2020)
30. Yao, L., Fang, C.H.: An automatic hardness measuring method using hough transform and fuzzy c-means algorithm. In: 10th IEEE International Conference on Fuzzy Systems.(Cat. No. 01CH37297). vol. 2, pp. 842–847. IEEE (2001)